Agricultural and Forest Meteorology 347 (2024) 109899

Contents lists available at ScienceDirect

Agricultural and Forest Meteorology

journal homepage: www.elsevier.com/locate/agrformet

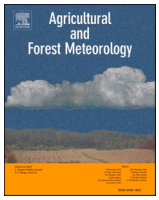

Boreal forest tree growth and sap flow after a low-severity wildfire☆

Paulina Dukat[a,b,*], Julia Kelly[c], Stefan H. Doerr[d], Johannes Edvardsson[e], Teemu S. Hölttä[a], Irene Lehner[c], Anders Lindroth[f], Cristina Santín[d,g], Natascha Kljun[c]

[a] Institute for Atmospheric and Earth System Research/Forest Sciences, Faculty of Agriculture and Forestry, University of Helsinki
[b] Meteorology Lab., Department of Construction and Geoengineering, Faculty of Environmental Engineering and Mechanical Engineering, Poznan University of Life Sciences, Piątkowska 94, 60-649 Poznań, Poland
[c] Centre for Environmental and Climate Science, Lund University, Lund, Sweden
[d] School of Biosciences, Geography and Physics, Swansea University, Swansea, Wales, UK
[e] Department of Geology, Lund University, Lund, Sweden
[f] Department of Physical Geography and Ecosystem Science, Lund University, Lund, Sweden
[g] Biodiversity Research Institute, Oviedo University, Mieres, Spain

ARTICLE INFO

Keywords:
2018 Drought
Eurasia
Forest fire
Nordic pine forest
Tree increment growth
Tree transpiration

ABSTRACT

Boreal forests are exposed to larger and more frequent fires due to climate change, with significant consequences for their carbon and water balances. Low-severity fires (trees charred but surviving) are the most common fire regime in the Eurasian boreal forest, but we still lack understanding on how they impact tree functioning. This study focused on the dynamics of tree transpiration and stem growth of *Pinus sylvestris* in central Sweden after a large wildfire in 2018. We compared a stand impacted by low-severity fire (LM) with an unburnt stand (UM), over three years following the fire (2020–2022). We found that transpiration was on average lower and more variable within the stand at LM compared to UM. LM also had consistently lower stem growth compared to UM, resulting in larger accumulated growth for the unburnt site in the second to fourth year after the fire. Our results highlight the complex effects of low-severity fire on tree water cycling, with both direct (damage to tree xylem and roots) and indirect fire impacts (due to loss of understory vegetation and changes in soil properties). Trees affected by low-severity fire also exhibited reduced resilience to water shortages. Considering the expected increase in frequency of droughts and forest fires at higher northern latitudes, such indirect fire impacts may put additional pressure on the boreal forest.

1. Introduction

Wildfires burn large areas of boreal forest each year, and thus play an important role in shaping the biodiversity, biogeochemical cycles and energy budget of this biome (Smith et al., 2011). As well as releasing significant amounts of carbon (C) during combustion, the direct impacts of fire such as the reduction of tree canopy, tree mortality and consumption of understory vegetation can lead to significant changes in the carbon uptake capacity of forests and their ability to store and use water (Faber-Langendoen and Davis, 1995). Wildfires increase the amount of rainfall reaching the ground and the surface runoff rate due to the consumption of vegetation while decreasing the infiltration rate due to changes in soil hydrophobicity (Tecle and Neary, 2015). Wildfires also alter evapotranspiration (ET), with an initial reduction due to the loss of vegetation and a subsequent increase due to plant regrowth (Vertessy et al., 2001; Nolan et al., 2014). Changes in the water cycle caused by fire have important implications for local to continental scale climate dynamics (Nolan et al., 2014).

Boreal forests across the globe are already experiencing larger and more frequent fires as a result of climate change (Zheng et al., 2023). Although they belong to the most broadly distributed biome where climate warming is strongest, boreal forest fires still receive less attention than fires in tropical forests (Zheng et al., 2023). A study of wildfire dynamics in a Siberian larch forest showed that climate-induced fire frequency and burned area are increasing in correlation with air temperature anomalies and drought occurrence (Ponomarev et al., 2016).

☆ Short summaryLow-severity fires are common across boreal Eurasia yet little is known about their impact on tree functioning. We find that low-severity fire leads to lower stem growth and often decreased transpiration in the surviving trees for four years after fire, highlighting the longevity of fire impacts.

* Corresponding author.
E-mail address: paulina.dukat@helsinki.fi (P. Dukat).

https://doi.org/10.1016/j.agrformet.2024.109899
Received 10 July 2023; Received in revised form 25 November 2023; Accepted 17 January 2024

During the last decades, the boreal forests of both North America and Eurasia experienced increased water deficit, resulting in an increase in fire-related carbon dioxide (CO_2) emissions (23 % of global fire CO_2 emissions in 2021; Zheng et al., 2023). Studies on the impacts of these fires on C and water cycling have mainly focused on high-severity (i.e. stand-replacing) fires in the North American boreal zone (Amiro et al., 2003; Girardin et al., 2006; Le Goff et al., 2007; Bremond et al., 2010; Walker et al., 2019). By comparison, Eurasian boreal forests have received very little attention, which limits the ability of policymakers to take informed decisions on sustainable forest management strategies in the face of increasing climate extremes and wildfire frequency. The Eurasian boreal forest fire regime is characterized by low-severity fires, which consume understory vegetation and small saplings but allow the continued survival of mature trees such as *Pinus sylvestris,* which are adapted to these types of fires (de Groot et al., 2013). However, there is limited knowledge on how low-severity fire affects tree growth, the C and water fluxes of the surviving trees, and the potential feedback to the climate and energy balance of these forests.

Low-severity fires can lead to temperatures higher than 300 °C near the bark surface (Flanagan et al., 2020). Hence, such fires may lead to tree injuries which impact whole-tree functioning and stem diameter growth especially if the xylem and cambial tissues are damaged (Bär et al., 2019). Balfour and Midgley (2006) analyzed the effect of heating on the xylem for Acacia *(A. karroo*) and showed that all heat-treated trees started shedding leaves immediately and experienced stem dieback within four weeks. Wildfire can damage xylem cell walls and lead to the formation of air bubbles (Michaletz et al., 2012; Partelli--Feltrin et al., 2022). Thus the tree canopy and xylem tissue can be damaged by embolism formation or xylem deformation if the heat transfer to tree tissue during burning is very high (Varner et al., 2021). Heat conduction through bark at a temperature of 60 °C can cause necrosis of the phloem and vascular cambium tissues (Bova and Dickinson, 2005; Michaletz et al., 2012). It has been shown for *Populus balsamifera* L. collected in Calgary, that heating leads to thermal softening of the viscoelastic polymers in the conduit walls (Michaletz et al., 2012). They deformed in response to the stresses caused by the hot air inflow. In addition, localized excessive heating during the fire can injure tree roots and canopy (Michaletz and Johnson, 2007; Michaletz et al., 2012). In some cases, soil temperatures during fire can rise to several hundred degrees, especially when there is deep combustion of the forest floor (Santín and Doerr, 2016). Such temperatures can impact the transport of xylem sap from roots to leaves, reduce phloem transport rate and reduce the growth of new tissues. In short, fire can affect tree diameter growth directly due to damage to tree tissues or indirectly if transport of water and nutrients around the tree is weakened by xylem and/or phloem damage.

To some extent, trees can recover from the damage caused by wildfire (Christensen-Dalsgaard and Tyree, 2014; Niu et al., 2017; Zeppel et al., 2019). Under certain conditions, low-severity fire can also have a positive impact on tree growth, as removed understory can result in temporarily decreased competition for water and nutrients (Peterken, 2001; Blanck et al., 2013). This in turn contributes to increasing tree carbon fixation and transpiration. For example, it has been reported for temperate coniferous forests in the US, that photosynthetic capacity was lower for burnt than for unburnt trees due to resource depletion (Bryant et al., 2022). Interestingly, for burnt trees, photosynthetic capacity increased with damage severity. Studies have shown that increasing photosynthetic efficiency at the leaf level can compensate for damage to entire trees, including loss of leaf and root area (Bryant et al., 2022).

Sap flow measurements, which record the rate of water transported through the tree sapwood, can provide important insights into the effect of fire on transpiration. Despite the versatility of sap flow data, few previous studies have measured sap flow on fire-affected trees. Ferrat et al. (2021) showed that tree sap flow in Mediterranean *Pinus nigra* stands in control and plots burnt by low-severity prescribed fire followed the same seasonal and daily pattern (Ferrat et al., 2021). Since leaf area reduction was low at the burnt plots, the fire did not lead to significant reductions in transpiration. In contrast, for moderate and high severity fires in a mixed species Australian eucalypt forest, Nolan et al. (2014) found that transpiration decreased 1–2 years after fire until the surviving trees grew new leaves (Nolan et al., 2014). At the ecosystem level, the growth of new seedlings partially compensated for the decreased transpiration during this period, favoring a faster recovery of evapotranspiration than if the forest would have regenerated from seedlings alone (without surviving mature trees). They also found that fire severity determined the effect of fire on ET, whereby average ET was 41 % lower in the forest burnt at high severity compared to an unburnt forest, but only 3 % lower at the low-severity burnt forest (Nolan et al., 2014).

In this study, we defined low-severity fire based on low tree mortality (<10 %) with charred trees but no direct foliage damage. The main aim was to assess how low-severity fire impacts tree growth and transpiration in a Nordic boreal forest. We examined (i) whether fire-affected trees could sustain similar sap flow to unburnt trees, (ii) how sap flow changed over time since the fire, and (iii) the impact of the fire on the stem diameter growth. We hypothesized (1) that transpiration and stem increment growth would be reduced in trees affected by low-severity fire due to possible xylem damage from the fire, even though the tree foliage was left intact; and (2) that the combustion of surface vegetation and soil organic layer impacted the regeneration on trees by changing the hydraulic properties of the soil.

2. Material and methods

2.1. Study area

The study area is located in the municipality of Ljusdal in central Sweden (61°56′ N, 15°28′ E). In July 2018, the Ljusdal area was hit by the second largest fire in Sweden in recorded history, burning a total of 8995 ha of forest. The fire was ignited by lightning strikes and spread quickly due to severe drought conditions. It burned primarily through coniferous forests, mainly Scots pine (*Pinus sylvestris*) with smaller areas of Norway spruce or birch. Our study area was composed of managed *Pinus sylvestris* forests on poor, sandy soil with understory vegetation dominated by mosses and lichens (*Cladonia* spp., *Pleurozium schreberi, Cetraria* sp. and *Polytrichum juniperinum*.) and small shrubs (*Vaccinium vitis-idaea, V. myrtillus, Calluna vulgaris,* and *Empetrum nigrum*), which is representative of the larger burnt and unburnt area. The 30-year mean annual air temperature in the area was 2.8 °C and the total mean annual precipitation 648 mm (1991–2020, national monitoring station Ytterhogdal, 40 km northwest of the study site; SMHI, 2022). We refer to Kelly et al. (2021) for a more detailed site description.

Here we compare two *Pinus sylvestris* sites (Fig. 1): a low-severity fire site where nearly 100 % of the trees survived one year after the fire (LM; Low-severity Mature) and an unburnt site (UM; Unburnt Mature). The sites cover approximately 4000 m^2. They are only 400 m apart and thus experience the same climatic conditions. Soil characteristics for both locations were very similar, with a shallow organic layer above sandy mineral soil. At LM, the tree charring height was 2.1 ± 0.2 m and the understory vegetation was completely consumed by the fire. This led to a loss of 0.93 kg m^{-2} forest floor biomass (based on post-fire comparison of UM and LM) with only 37 ± 2 mm of the total organic layer remaining at LM, compared to the (organic) florest floor depth of 149 ± 4 mm at UM (Kelly et al., 2021). The tree canopy at LM was not scorched during the fire, i.e. the needles remained green, and visual inspection of the tree trunks did not reveal any injuries except for charring of the outer bark by the fire. The LM stand had a tree density of 484 trees ha^{-1}, an average tree height of 19.3 ± 0.5 m and an average diameter at breast height (DBH) of 24 ± 2 cm. The UM stand had 688 trees ha^{-1}, an average tree height of 15.3 ± 0.4 m, average DBH of 20 ± 1 cm (Figure S1).

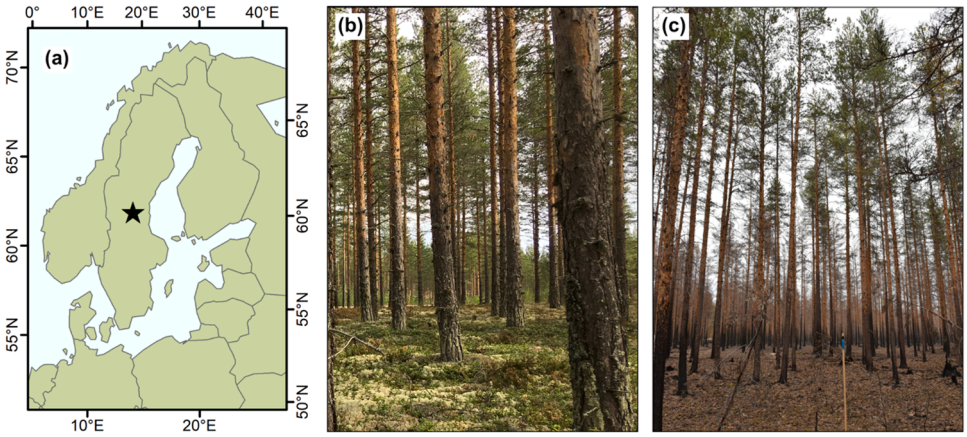

Fig. 1. a) Location of the study area within Sweden. Photos of the sites taken in 2019: b) Unburnt Mature (UM), and c) Low-severity Mature (LM). Map source: © Lantmäteriet, Sweden.

2.2. Meteorological measurements

Climate data for the study area was collected in an open area 400 m away from the two forest stands. Precipitation for June-September was measured with an ARG314 (EML, UK) and gap filled for the remaining months with data from a national monitoring station (Sveg A, 60 km east from the study area, 357 m a.s.l., (SMHI, 2022)). Incoming, above canopy photosynthetically active radiation (PAR) was measured with a full-spectrum Quantum sensor (SQ-500-SS, Apogee Instruments). At each site, air temperature and humidity were monitored at 2 m height with a HygroVUE^{TM} 10 (Campbell Scientific, Inc., USA) and used to calculate water vapour pressure deficit (VDP). In this study, we used soil temperature and volumetric water content measured at 7.5 cm depth at three locations at each site to capture the spatial variability (CS655-DS sensors, Campbell Scientific, Inc., USA).

2.3. Sap flow measurements

Sap flow was derived using the tissue heat balance (THB) method, where the rate of water transport through the xylem is calculated from the power consumption and the temperature increase of the water passing through the stem (Čermak et al., 1973; Čermák and Deml, 1974; Kucera et al., 1977). The thermal balance is derived for an area of the water conducting stem heated by 3 electrodes (Obojes et al., 2018; Szatniewska et al., 2022b). The recorded input energy is split between conductive heat losses and advective transport of heat with the xylem sap flow (Čermák et al., 2004). The THB method has been shown to be nearly independent of the sap flow radial profile (Kučera, 2018). Whole tree sap flow rate [kg time^{-1}] was derived by multiplying sap flow (Q [(kg cm^{-1} time^{-1})]) with tree circumference (Ci [cm]), after excluding the thickness of the bark and phloem layer (B [cm]) (Szatniewska et al., 2022a). The flow rate of sap per unit sapwood area (sap flux density) for each tree (SF [kg cm^{-2} day^{-1} and g cm^{-2} h^{-1}]) was then calculated by dividing the tree sap flow rate by the sapwood area (A [cm^{-2}]):

$$SF = \frac{Q(Ci - 2*\pi B)}{A} \quad (3)$$

In August 2019 (i.e. one year after the fire), sap flow sensors (SF 81, Environmental Measuring Systems s.r.o. EMS Brno, Czech Republic) were installed at breast height at 6 representative trees per site. Here, we present measurements during the growing seasons (May to October) 2020, 2021 and 2022. At the start of the 2021 measuring season, sensors at two trees at the UM site had to be moved to new trees due to resin accumulation, and in 2022 the same occurred for one tree at LM. The dimensions of the trees with sap flow sensors are presented in Table 1. The zero transfer value of sap flow, i.e. the "baseline" at which no transpiration is assumed to occur, was obtained using the exponential weighting method with a 5 days averaging period, as described in Kučera (2018) and Kučera et al. (2020). Note that in the following, we used the terms "sap flow" to refer to the xylem water flow process, "sap flow density" to represent sap flow per sapwood unit area, and "transpiration" for the cumulative sap flow on a daily timescale.

2.4. Dendrometer measurements

Changes in stem circumference were measured at 2 m height by dendrometers (DR26E, EMS Brno, Czech Republic) on the trees with sap flow sensors. The circumference was measured with a resolution of 0.002 mm every 5 min and allowed for the exact tracing of even small DBH changes. The dendrometer measurements were available from April or May to October in 2020–2022, i.e. not including the winter months. The dendrometer bands were however left on the trees all year round. To estimate the stem increment and its phases for each year, dendrometer data from all trees were averaged for each site. The typical pattern of annual tree diameter growth reported in the literature

Table 1
UM (Unburnt Mature) and LM (Low-severity Mature) sap flow tree characteristics. Sensors at UM trees 2 and 6 were moved to new trees at the start of 2021 and LM tree 5 was also replaced in 2022. Sapwood area [ha^{-1}] was calculated using the number of trees ha^{-1} and the relationship between DBH and tree sapwood area (Fig S1).

Unburnt Mature (UM) site				Low-severity Mature (LM) site			
Tree	DBH (cm)	Thickness bark + phloem (cm)	Sapwood area (m^2)	Tree	DBH (cm)	Thickness bark + phloem (cm)	Sapwood area (m^2)
1	26	0.7	0.052	1	23	0.7	0.039
2	18/16	0.6/0.6	0.024/0.019	2	18	0.4	0.023
3	22	0.5	0.036	3	34	0.6	0.090
4	25	0.5	0.049	4	30	0.7	0.067
5	18	0.8	0.022	5	27/27	0.5/0.5	0.055/0.055
6	23/23	0.7/0.7	0.039/0.039	6	22	0.4	0.038
Sapwood area ha^{-1} (2020)			16.50	Sapwood area ha^{-1} (2020)			17.32

(Zweifel et al., 2010; Dukat et al., 2021) guided the determination of the growth phases in this study. Five phases in stem circumference were determined for each year: (i) the maximum winter contraction (MWC) phase in late winter when the minimum stem diameter is reached due to freezing and tissue dehydration (Mayr et al., 2007; Zweifel et al., 2010); (ii) the rehydration period (rP) when tree stem increment recovers from the MWC to the level at which tree growth had stopped in the previous autumn; (iii) the main radial growth period (RGP); (iv) the low radial growth period when reversible stem shrinkage and expansion relate mainly to the changing stem water content and soil conditions (especially drought) (WT) and finally, (v) the phase at the end of the growing season, when large reversible stem shrinkage and swelling may occur due to reduced precipitation and freezing temperatures (PS). The initial point of tree growth (L0) was determined as the stem circumference measured in late autumn of the prior year (Deslauriers et al., 2007). Previous studies have shown that during the spring, the maximum stem contraction is reached, therefore, the increase in stem diameter from the lowest records in the spring cannot be considered as the growth starting point, as it is only a reversible swelling due to refilling of tree internal water stores (Kolari et al., 2014; Dukat et al., 2021; Zweifel et al., 2010).

2.5. WUE at tree level

Tree water use efficiency (WUE [kg^{-1}]) was calculated as tree-level dry biomass production [kg] per total tree level transpiration [kg] from the period of biomass growth. The dendrometer measurements were used to define the period of wood growth. We used an allometric equation for Sweden developed by Marklund (1988) and updated by Petersson and Ståhl (2006) to estimate the tree dry biomass increment per year. Tree level total transpiration within this period was based on the sap flow measurements. WUE was calculated as the site average of all available sample trees for a given year.

2.6. Tree-ring width chronologies

As a complement to the dendrometer measurements, we took tree cores from 5 trees at each site to examine the tree growth before and after the fire. The increment cores were analysed and data processed following standard dendrochronological procedures (Bräker, 2002). Tree-ring widths (TRW) were measured to the nearest 0.01 mm using a digital LINTAB positioning table connected to an Olympus stereomicroscope and TSAPWin Scientific software (Rinn, 2003). Prior to standardization, all TRW series were cross-dated for missing rings and dating errors using COFECHA (Cook and Holmes, 1984). To minimise the influence of non-climatic variations and trends, related to e.g., tree age and geometry, the TRW series were standardized and transformed into dimensionless indices (Fritts, 1976; Cook and Kairiukstis, 1990) using ARSTAN_41d (Cook and Krusic, 2006). As non-significant synchronism was detected between the burnt and unburnt pine trees, and to preserve potential low-frequency variations in the tree growth, a flexible Friedman's variable span smoother (Friedman, 1984) was used for standardization.

2.7. Ancillary vegetation measurements

We quantified the recovery of the understory vegetation since the fire based on vegetation surveys at LM and UM. We surveyed 12 quadrat plots of 25 × 25 cm along two transects at each site in July 2020 (Delin, 2021) and 2022. We visually estimated the percentage of ground covered by each vascular and bryophyte species present in the quadrat.

The effective plant area index (PAI_e) was used to estimate changes in tree canopy coverage since the fire at both sites. PAI_e was derived from upward-facing hemispherical photos using a 180° fisheye lens. Three photos were taken at three points at each site once per year at the end of the growing season. We use the term PAI_e instead of LAI (leaf area index) to clarify that tree stems and branches visible in the photos were included in the calculation of the plant area. The photos were first processed in MATLAB (v.2020a) using histogram matching to ensure a similar brightness between images and then binarized to separate sky from vegetation using an adaptive threshold function. The binary images were processed in CAN-EYE (v.6.4, INRAE, France) to calculate effective PAI, i.e. PAI_e based on the assumption that the foliage is randomly distributed.

3. Results

3.1. Meteorological conditions

The meteorological conditions at the study area are presented in Fig. 2 and the site-specific soil moisture and temperature data during the growing season are shown in Fig. 3. We defined the growing season as May 1 to October 15 because this is when daily mean soil temperature (Tsoil) at 7.5 cm depth was $\geq$ 5 °C at both sites. However, it should be noted that soils reached this threshold between 2–21 days earlier and for up to 19 days longer at LM than at UM.

The average growing season air temperature (Tair) was lowest in 2020 with 11.3 °C and highest in 2022 with 12.0 °C. Nevertheless, during a short period in June 2020, air temperature, incoming PAR (photosynthetically active radiation) and VPD (water vapor pressure deficit) were all higher than in any other year (Fig. 2a, c, d). The growing season precipitation sum was also lowest in 2020, totaling 332 mm. In 2021 and 2022, the total growing season precipitation was 369 mm and 434 mm, respectively (Fig. 2b). During the summer months (i.e. June-August), mean daily air temperature reached 15.0 °C, 15.4 °C and 16.0 °C in 2020, 2021, and 2022 respectively. In 2020, the highest monthly precipitation was measured in July (118 mm), while only 23 mm were recorded in August. In 2021, precipitation was relatively equally distributed over the summer months whilst in 2022 the highest precipitation was recorded in August (154 mm).

The volumetric soil water content (VWC) during the growing season was higher at LM than at UM in 2020 and 2021 (Fig. 3a-b). However, in 2022, VWC was higher at UM until mid-July, and then similar at both sites during the following months (Fig. 3c). During the growing season, soil temperature (Tsoil) was generally higher at LM than at UM (Fig. 3d-f). The mean growing season Tsoil was 11.0–11.6 °C at LM and 9.3–10.4 °C at UM. In 2022, Tsoil at LM reached 5 °C almost a month earlier than at UM.

3.2. Sap flow dependence on environmental conditions

At the start of the 2020 growing season (May-June), sap flux density (transpiration) was higher at LM than at UM (Fig. 4a), likely due to the higher soil temperatures at LM where soils thawed earlier than at UM (Fig. 3d). From July until mid-August 2020, sap flux density was substantially higher at UM compared to LM. After mid-August, sap flux density declined at both sites, corresponding with a period of no growth and even shrinkage of tree stems (Fig. 7) as well as very low soil moisture (Fig. 3a). At the end of the growing season, similar daily cumulative sap flow rates per sapwood area were measured at both sites. In 2021, both sites had similar mean daily sap flux density, especially during the start and end of the growing season. In July and August there were two periods when the sap flux density at LM was slightly higher than at UM. In 2022 (four years after the wildfire), we observed the largest difference in sap flux density between the sites, with substantially lower sap flux density at LM than at UM throughout June, July, and August (Fig. 4c). Even if the two sites had partly similar mean hourly sap flux density, e.g., in June 2020 and 2021, the sap flux density range among the trees was much larger at LM than at UM (Fig. 5).

To assess the relationships between the meteorological factors and the sap flow at a higher temporal resolution, the hourly sap flux density from all available trees were binned in equal intervals based on the value of a given meteorological factor (Fig. 6). Using hourly data allowed a

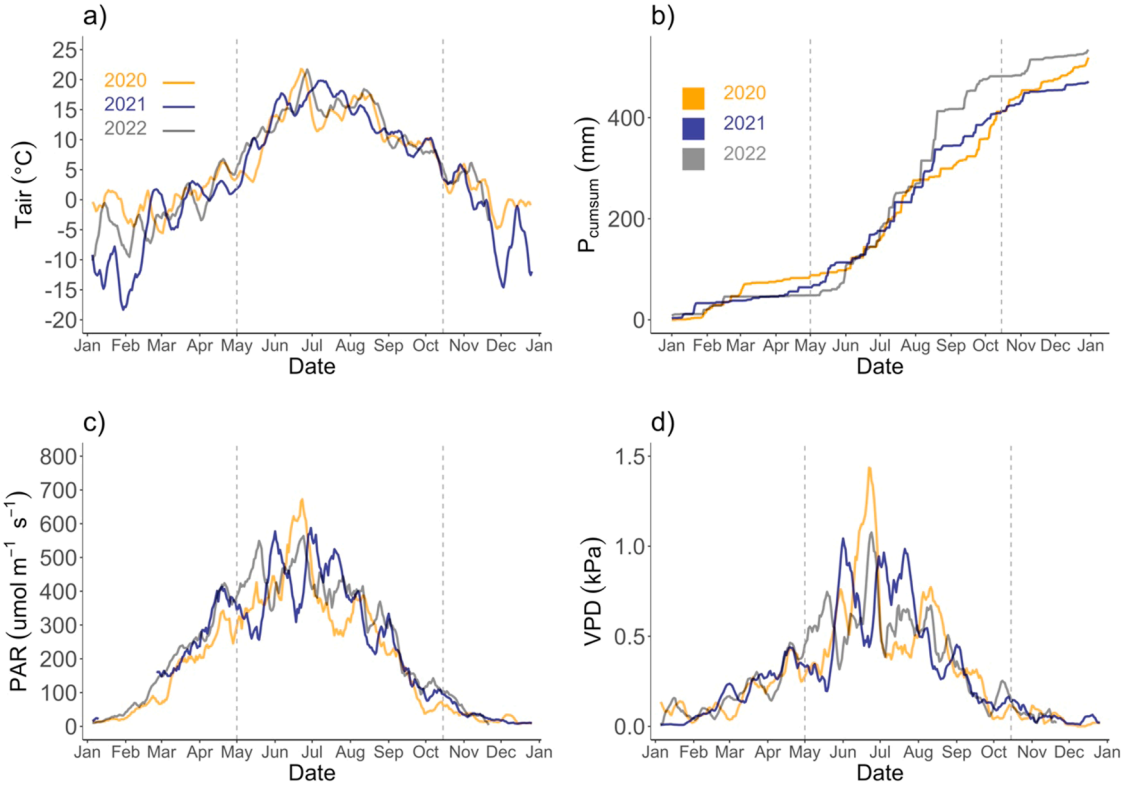

Fig. 2. Daily means of meteorological conditions at the study area for 2020–2022. The panels show a) air temperature (Tair), b) cumulative precipitation (P_{cumsum}), c) incoming photosynthetically active radiation (PAR), d) water vapor pressure deficit (VPD). A 10-day moving average was applied to the data in panels a), c), and d). The gray dashed vertical lines indicate the growing season (May 1 to October 15).

better understanding of the responses of the trees to fast changing environmental conditions at the sub-daily scale. Transpiration (i.e. sap flow) is driven by soil water availability (VWC), water vapour deficit (VPD) in the air (evaporative demand), and available energy (PAR). This analysis showed that the responses of the trees to environmental conditions varied with regards to site and year of measurement (Fig. 6). Nevertheless, in all cases the UM site tended to have higher mean sap flux density at a given level of an environmental variable than LM.

Sap flux density was highest at soil moisture (VWC) values of 0.06–0.08 m^3m^{-3} for both sites during all years and declined as the soil became wetter or drier. LM had lower sap flux density rates than UM for any given VWC value. The response of sap flow to VPD at both sites was similar in all years, with a sharp increase in sap flux density as VPD increased from 0.5 to 1 kPa and saturation at around 1.5 kPa. Sap flux density increased with increasing soil temperatures at both sites, suggesting that soil temperature was not a limiting factor for sap flow. As expected, a clear response of sap flux density to light (PAR) was observed for both sites, with saturation of sap flux density at high PAR (>1400 μmol m^{-2} s^{-1}).

3.3. Seasonal and annual stem increment growth

All trees with sap flux density measurements were also equipped with a dendrometer to record hourly variations in stem size which we used to estimate the annual stem growth of the trees (Section 2.4). Daily averages of measurements from all trees per site allowed us to compare the total annual stem radial increment (Ri) between sites and years (Fig. 7). For all years, total annual Ri was smaller at LM than at UM. The total annual Ri at UM was 0.13 cm in 2020, 0.30 cm in 2021 and 0.27 cm in 2022, (Table 2). At LM, total Ri was also relatively high in both 2021 and 2022 (~ 0.27 cm and 0.21 cm, respectively), whereas in 2020 there was almost no growth (0.07 cm). 2021 was the year with the smallest difference in total Ri between the sites (Fig. 7 b). It was also the only year when Ri during the maximum winter contraction (MWC) was lower at UM than at LM. During all measured growing seasons and at both sites, short-term reversible stem swelling was associated with the occurrence of precipitation and fluctuations of soil water content (particularly during the second half of the growing season). In 2020, the response to these changes was much stronger at UM than at LM (Fig. 7a), whereas in the following two years the response was similar at both sites (Fig. 7b, c).

3.4. Water use efficiency (WUE)

WUE at tree level was visibly lower for LM than for UM in 2020 and 2022 (Table 2). WUE was at its highest level in 2021 for both sites. In 2022 WUE dropped at both sites compared to 2021. At LM, the total average tree transpiration [kg] of the radial wood growth period also dropped, while it increased at UM. The highest total tree biomass growth per hectare occurred in 2021 at LM and in 2022 at UM.

3.5. Tree ring widths

The tree ring width (TRW) index chronologies shown in Fig. 8 provide a longer-term perspective on the tree growth at the UM and LM sites during the four decades before the fire as well as in the years that followed. The chronology from the UM site covered the period 1965–2021 and all trees were estimated to be between 60–70 years old. The chronology at the LM site covered the period 1902–2021 with two trees around 130 years old and the remaining trees around 90 years old, which is 20 years older than a previous estimate for the site and reflects the larger variability of tree DBH at LM compared to the UM (Kelly et al 2021, Figure S1). Note that the tree cores were taken from other trees than the sap flow measurements. The correlation between the standardized chronologies at the two sites was r = 0.40 but increased to 0.54 for the residual chronologies (corrected for autocorrelation). Between 1965 and the mid-1990s, correspondence between the chronologies was

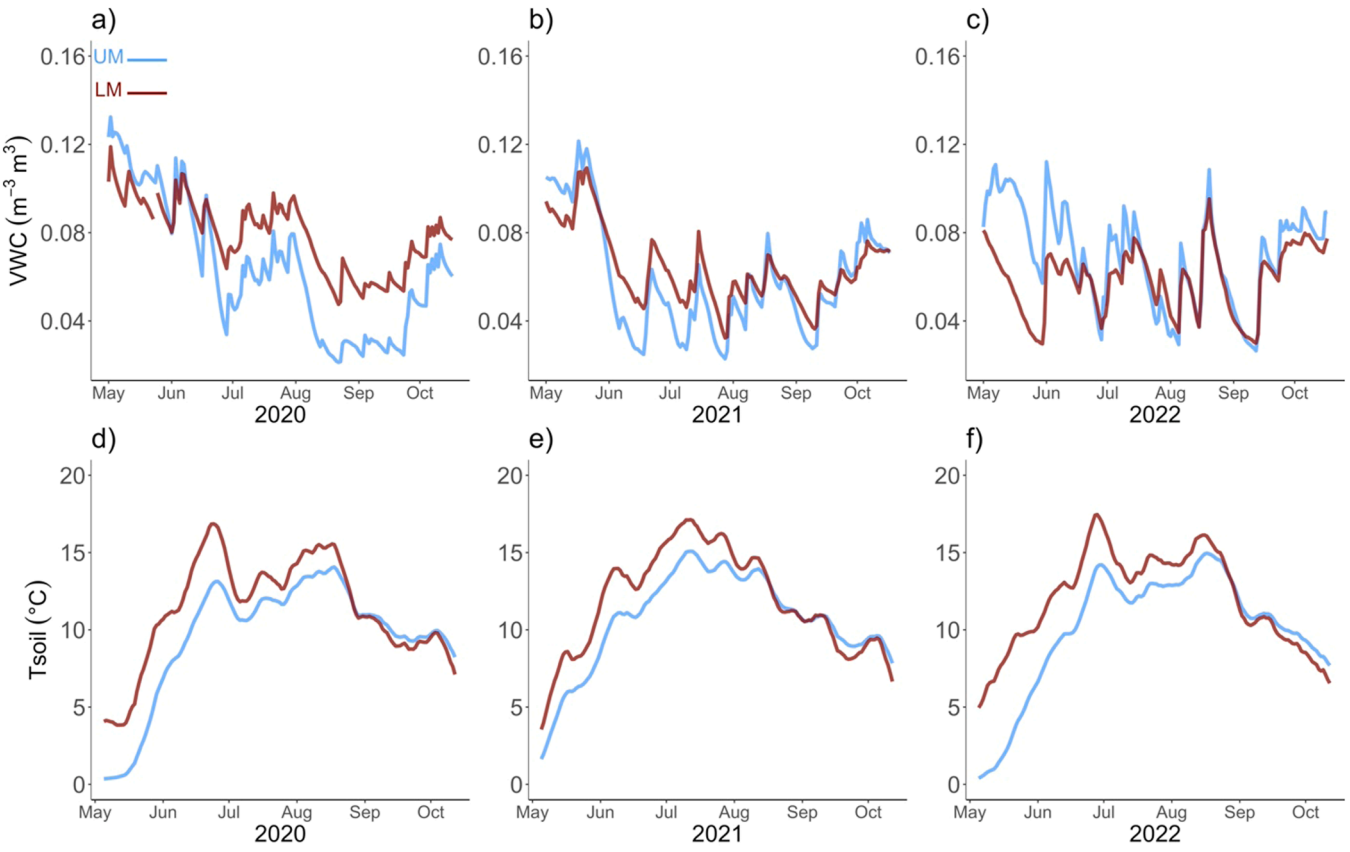

Fig. 3. Daily means for 2020–2022 of a-c) volumetric soil water content (VWC), and d-f) soil temperature (Tsoil) at 7.5 cm depth, at the UM site (blue) and the LM site (red).

low, followed by several consecutive years of lower growth at the LM compared to UM (1996–2003). However, since 2010, the trees at both sites have shown similar growth patterns, until the fire in 2018. In the year of the fire, the UM tree growth declined substantially (TRW index = 0.50) and was lower than for any other year in the preceding four decades, whilst at the LM, tree growth also decreased but was just below the mean (TRW index = 0.93). For the years following the fire, the growth rate of the UM trees returned to equal or above mean TRW values, whereas radial growth continuously declined at LM. A comparison of the average TRW index value for the 3 years before and after the fire reveals a 9 % increase in growth at UM after the fire whereas the TRW index at LM declined by 72 % after the fire.

3.6. Understory vegetation cover and plant area index

In 2022, the understory and forest floor vegetation at UM covered most of the soil surface (total cover = 92 %) and was dominated by bryophytes (68 % mean cover compared to 24 % for vascular plants). The only vascular species recorded were *Vaccinium vitis-idaea* (appeared in all plots) and *Calluna vulgaris* (83 % plot occupancy). *Cladonia sp*. was the most common bryophyte (appeared in all plots) followed by *Pleurozium schreberi* (83 % plot occupancy), then *Polytrichum juniperinum* and *Cetraria* sp. (both 17 %). At LM, the average cover of vascular vegetation increased from 9 % in 2020 to 20 % in 2022 whilst bryophyte cover increased from <1 % to 6 % in 2022, giving a total vegetation cover of 26 % four years after the fire. The most common vascular species at LM in 2022 was *Vaccinium vitis-idaea* (83 % plot occupancy), followed by *Pinus sylvestris* seedlings (17 %) and by *Betula* sp., *Vaccinium myrtillus*, and *Calluna vulgaris* (all with 8 % plot occupancy). *Vaccinium vitis-idaea* and *Calluna vulgaris* were the only vascular species present in 2020. *Polytrichum juniperinum* was the most common bryophyte in 2022 (33 % plot occupancy) followed by *Cladonia sp*. and *Pleurozium schreberi* (both 17 %).

There was no significant difference in the effective Plant Area Index (PAI_e) between the sites or among years. PAI_e was on average 0.66 ± 0.03 and 0.64 ± 0.02 at the UM and the LM site, respectively. This result confirms that the tree canopy at LM was not visibly affected by the fire.

4. Discussion

4.1. Response of sap flow to post-fire conditions

In this study, we investigated the impacts of a low-severity fire on tree radial growth and sap flow in a managed boreal forest of *Pinus sylvestris* in Sweden, by comparing trees in a fire-affected area with trees in an adjacent unburnt stand. The trees at both sites had similar total sapwood area and thus similar transpiration fluxes would be expected if the trees had not been damaged by the fire. We hypothesized that trees affected by the fire (LM stand) would have lower transpiration than trees from an unburnt stand (UM) due to fire-related injuries. When analysing hourly sap flux density as a function of VWC, soil temperature, or PAR (Fig. 6), we found that sap flux density at LM was lower than at UM during the whole study period. However, we did not observe consistently lower transpiration in the time series of LM compared to UM. Specifically, transpiration was reduced at LM compared to UM during July and August in the second year after fire and throughout the growing season of the fourth year after fire, but in the third year, transpiration was similar at both sites (Fig. 4). The maximum daily transpiration rate was 18 % lower at LM than at UM in 2020 and 36 % lower in 2022. The decreased transpiration at LM in 2020 (second year after fire) is likely to be an effect of the fire. However, it is more difficult to disentangle the impact of the fire on the transpiration of the LM trees in 2021 and 2022.

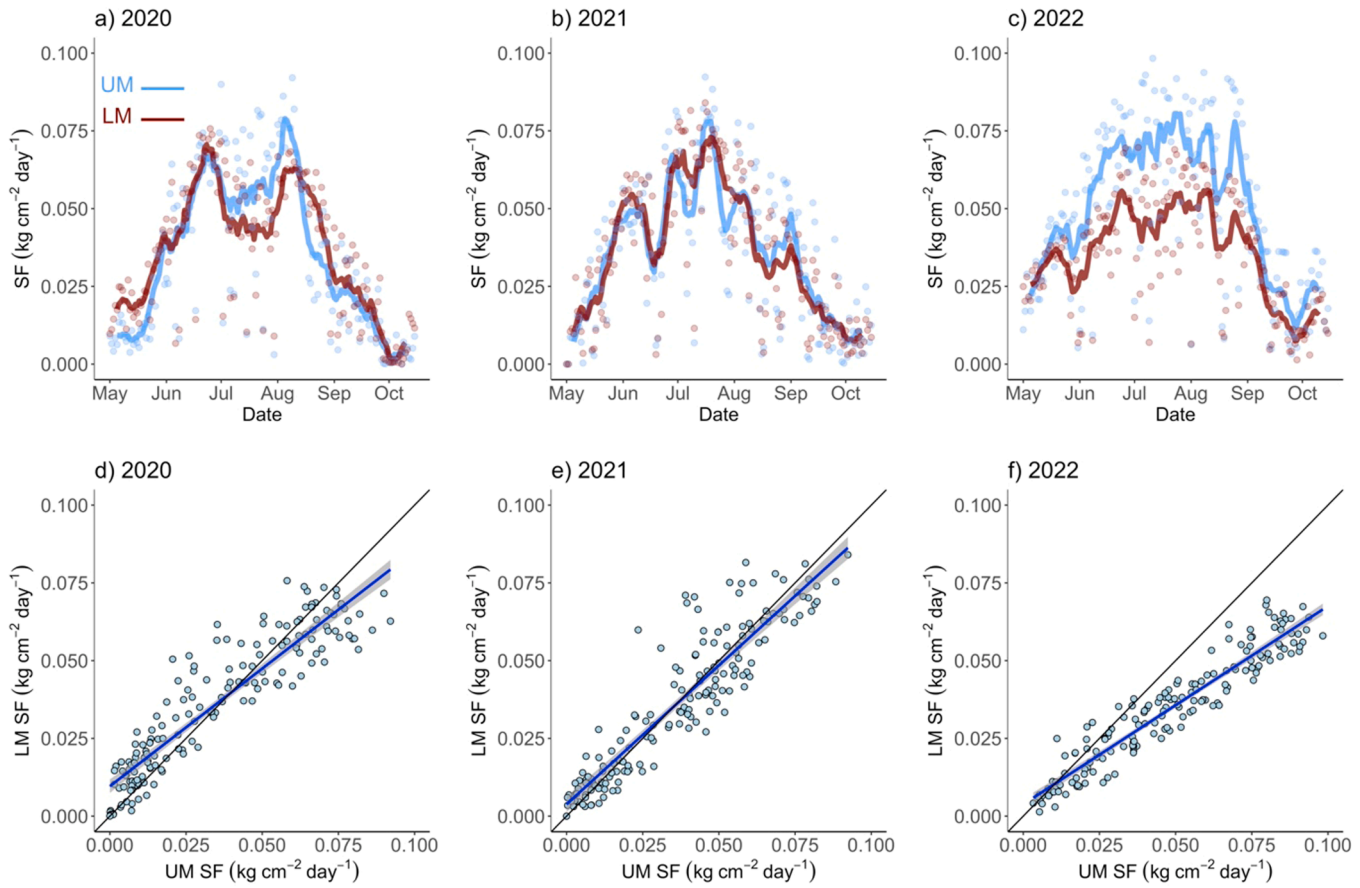

Fig. 4. Daily sap flux density averaged in 10-day moving windows (solid line) for the Unburnt Mature (UM; blue line) and the Low-severity Mature (LM; red line) sites for 2020–2022 (a-c). Direct comparison of cumulative daily sap flux density measured at UM and LM for 2020–2022 are shown in d-f. The black line denotes the 1:1 line and the blue line is a linear regression with 95 % confidence intervals.

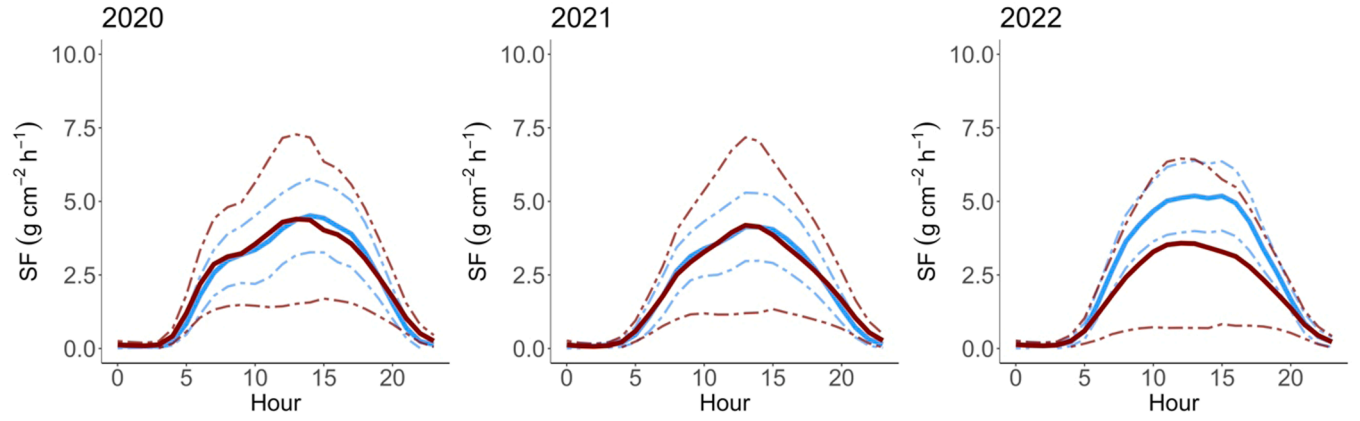

Fig. 5. Daily patterns of average hourly sap flux density (SF) for all trees for June 2020–2022, at the Unburnt Mature (UM, blue) and Low-severity Mature (LM, red) sites. The solid line is the site average, dashed lines show the standard deviation.

If the influence of other factors (e.g. meteorological conditions), including those indirectly caused by the fire (e.g. changes in soil moisture, changes in undergrowth vegetation), becomes important in time then they may significantly contribute to the variability of transpiration together with the direct tree-fire damage.

There are several mechanisms that can explain why the LM trees showed reduced sap flow compared to unburnt trees at UM two years after the fire. Although low to medium intensity fires often do not pose an immediate lethal threat to mature, fire-tolerant trees, they can cause a variety of injuries that disrupt the functioning of the entire tree (Bär et al., 2019). For example, the lower sap flux density at the LM site may be due to xylem cavitation and/or thermal damage to the tree trunks during the fire (Renninger et al., 2013). In more severe cases, tree trunk burning can result in a sufficient increase in temperature in the cambium to cause damage and death to living tissue. If the damage is extensive enough, it can lead to whole-tree mortality (Peterson and Ryan, 1986; Ducrey et al., 1996; Dickinson and Johnson, 2001; Butler et al., 2005), but this was not the case at our low-severity fire site. *Pinus sylvestris* is adapted to low-severity fire - its thick bark protects the cambium from fire-related damage (Uhl and Kauffman, 1990); and we did not note any

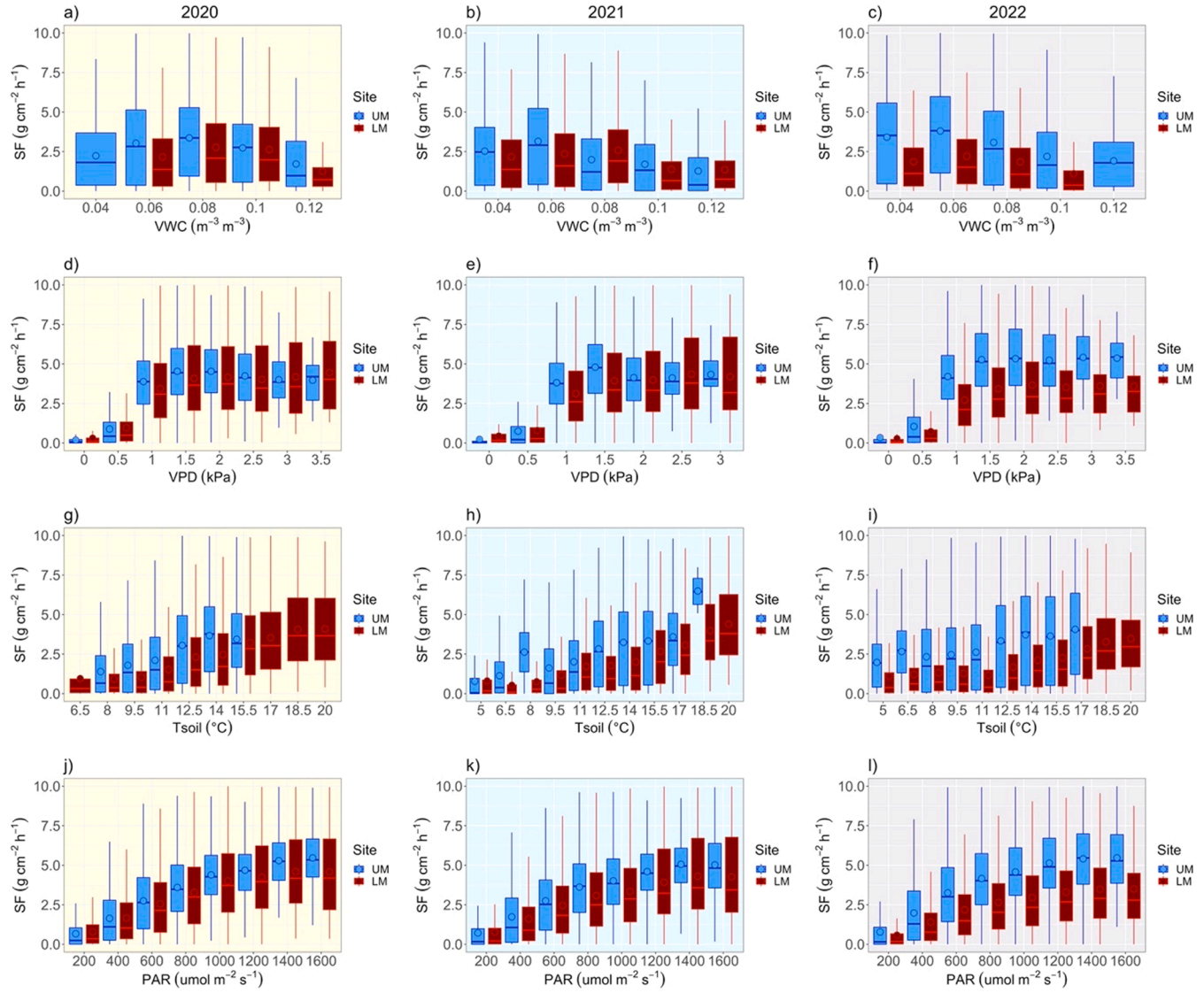

Fig. 6. Box plots, including median (circle) and average (line) showing the hourly tree sap flux density SF) in response to volumetric soil water content (VWC - a, b, c), vapour pressure deficit (VPD - d, e, f), soil temperature (Tsoil – g, h, i), and photosynthetically active radiation (PAR – j, k, l) for the 2020–2022 growing seasons at the Unburnt Mature (UM) and the Low-severity Mature (LM) sites. Measurements during precipitation (> 0.2 mm per half hour) were excluded, as then sap flow is near zero.

obvious injuries to the tree trunks at LM except for charring of the bark.

Nevertheless, even low-severity fire can lead to damage of shallow fine roots, especially if there is significant consumption of the forest floor. (Swezy and Agee, 1991) reported for old-growth *Pinus ponderosa*, that fire decreased the biomass of fine-roots (dry weight) by 50–75 % depending on fire severity. Almost half of *Pinus sylvestris* fine root biomass is located within the forest floor layer (Persson, 1980; Vanguelova et al., 2005). This layer was mostly consumed by the fire at LM, suggesting that the LM trees may have lost a substantial portion of their fine root biomass. This loss is significant as fine roots are capable of accessing water and nutrients over vast areas (Valverde-Barrantes, 2022). The loss of the fine roots may also explain the reduced radial growth observed in the TRW data for the LM trees after the fire (Fig. 8).

A reduction in transpiration may be an adaptation mechanism to prevent water potentials from decreasing too low as the fire could have decreased the water uptake capacity of the trees due to loss of fine roots and/or the xylem hydraulic conductance due to embolism and/or xylem deformation. For example, West et al. (2016) have shown both experimentally and theoretically, that hydraulic failure occurs during fire-induced heat waves (West et al., 2016).Thus, post-fire damage assessments should consider possible hydraulic impacts and limitations to water access in conjunction with the direct effects of heat transfer during fire (Bär et al., 2018). It have shown, that trees have the capability to recover from embolism, thus variations in tree functioning related to disturbance should be monitored over several years to capture the net effect of the disturbance been (Zeppel et al., 2019).

We cannot exclude the risk of future negative impacts to tree health and growth resulting from indirect effects of the fire, such as limited carbon and water fluxes or increased vulnerability to insect attacks, pathogenic infections and extreme weather events (Bär et al., 2019). The substantially lower sap flux density at the LM site measured in 2022 may be due to such longer-term, indirect fire impacts emerging at LM. Such factors can cause latent post-fire tree mortality even for initially healthy trees. The transpiration reduction in LM in 2022 may also be a response to post-fire changes in soil temperature and soil moisture availability due to the fire (see Section 4.2). It is also important to highlight that the within-stand variation of hourly sap flux density was larger at LM than at UM, for all measured years (Fig. 5). This increased variability at LM may result from the wider range of tree diameters at the stand scale compared to UM or individual features of the trees (like bark thickness), but it

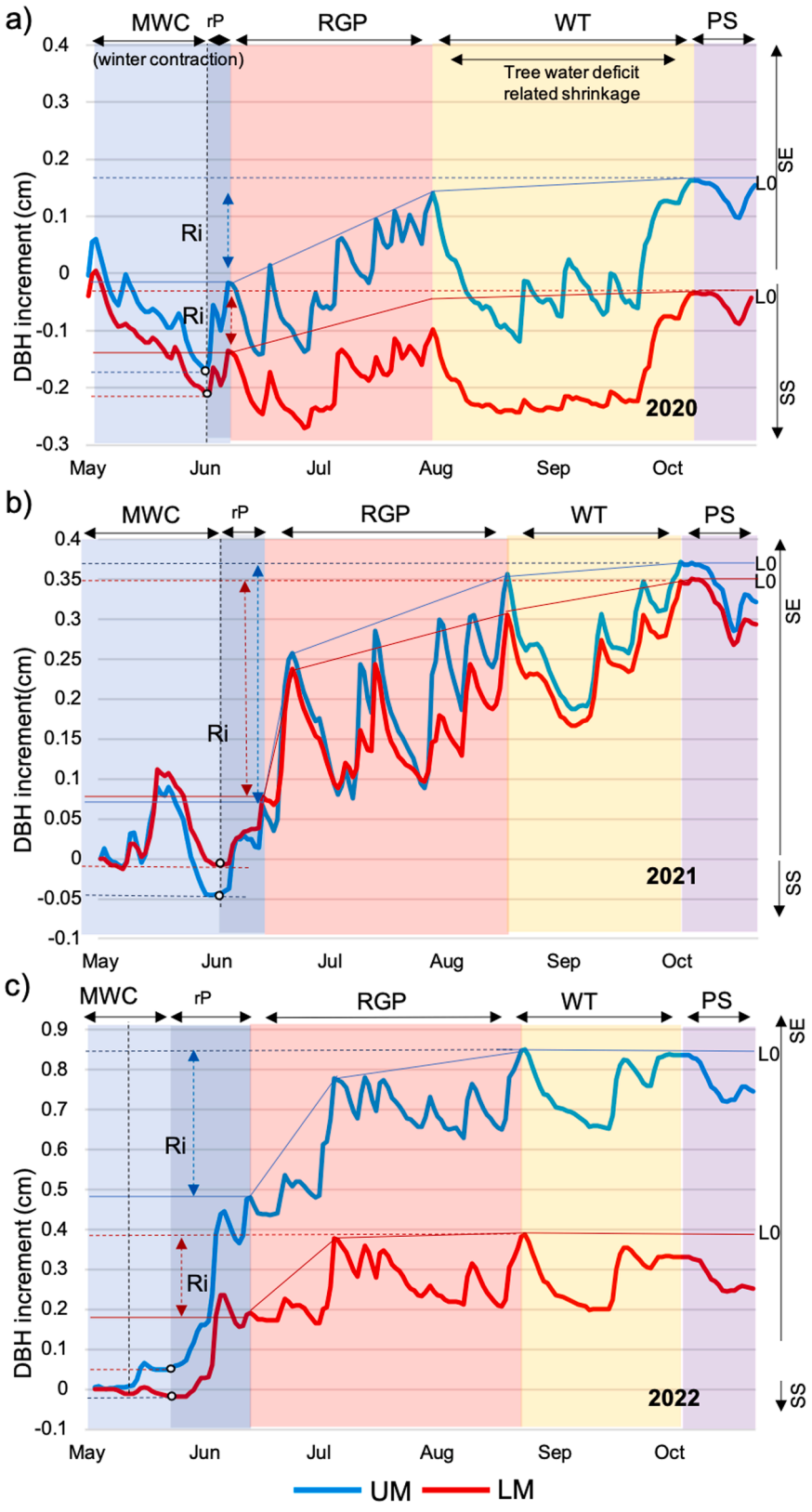

Fig. 7. Cumulative daily stem increment at 2 m height for all sap flow trees for a) 2020, b) 2021, and c) 2022 at the Unburnt Mature (UM, blue line) and the Low-severity Mature (LM, red line) sites. Note the different y-axis scales in each subplot. Ri denotes the stem increment, MWC is the period which ends with the maximum winter contraction (the peak of MWC is marked with a white point), rP is the rehydration period, RGP is the radial wood growth period, WT is the period with low increment expansion related to wood growth, with reversible stem shrinkage and swelling mainly related to water transport dynamics within the tree, PS is the post-growing season phase without growth (only reversible swelling and shrinkage), L0 is the zero line used to designate the start of stem increment for the next growing season, SE denotes stem expansion, and SS stem shrinkage. Description after Zweifel et al. (2010).

Table 2
Increment of diameter at breast height (DBH [cm]), dry biomass increment at tree [kg] and stand scale [t C ha^{-1}], total transpiration [kg] as well as water use efficiency (WUE) at tree level, for the Unburnt Mature (UM) and Low severity Mature (LM) sites in 2020, 2021, and 2022. Total transpiration was calculated for the radial wood growth period (RGB), i.e. 17/06–01/08 2020, 17/06–21/08 2021, and 15/06–23/08 2022.

Site	Year	Average DBH increment (cm)	Average tree dry biomass increment (kg)	Total RGP transpiration for average tree (kg)	WUE at tree level [-] (10^{-3})	Total stand biomass increment (tC ha^{-1})
UM	**2020**	0.17	2.35	986	2.38	1.62
	2021	0.30	4.31	1179	3.66	2.96
	2022	0.37	5.45	1556	3.50	3.75
LM	**2020**	0.07	1.30	1121	1.16	0.63
	2021	0.27	4.72	1404	3.36	2.28
	2022	0.21	3.77	1270	2.97	1.83

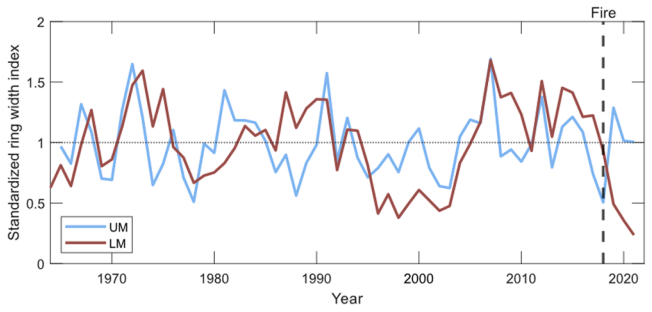

Fig. 8. Average standardized tree ring width index (dimensionless) chronologies for the UM and the LM sites. The dashed line in 2018 shows the date of the Ljusdal fire, and the dotted line represents the chronology mean.

could also indicate differences in fire exposure. The effect of fire on vegetation depends on the temperature and duration affecting different parts of the plant, which are the result of fire behavior variables such as the intensity of the fire line, flame height and the residence time (Michaletz and Johnson, 2007). Thus, variations in fire behavior within the LM site may have resulted in some trees having suffered more severe damage than others, leading to larger declines in transpiration without causing mortality. On the other hand, the relationship between transpiration and environmental factors (Fig. 6) remained similar for both sites across the three years (although the absolute values of transpiration were lower at LM than UM). In particular, the responses to VPD and light availability suggest that LM trees have maintained their functioning, despite reductions in transpiration.

The within-stand variation of sap flux density points to the fact that a larger amount of dendrometer and sap flow sensors might have reduced the uncertainty of allocating the impacts of the fire. Even though the number of dendrometer sensors is in line with the high standards of the ICOS protocol (Gielen et al., 2018) our findings show that with the local variability of fire behaviour, future studies could profit from an increased sampling size and replicates of each treatment (low-severity fire and unburnt).

4.2. Changes in soil temperature and water availability

Fire not only impacts trees directly, but also alters their environment by burning the understory vegetation and the organic soil layer, which changes soil water availability and soil temperature for many years after fire. At the LM site, 83 % of the forest floor layer was consumed by the fire (relative to UM). By the fourth post-fire growing season, the understory vegetation at LM had only reached a quarter of the cover of that observed at UM, and the plant composition differed considerably (less bryophyte cover, fewer bryophyte species and larger diversity of vascular plants at LM). As a result of reduced insulation by the forest floor and understory vegetation, the soil at LM was exposed to larger soil temperature variability than that at UM. One year after wildfire, hourly soil temperatures have varied between -8 and 0.1 °C during winter (Jan-Mar, not shown) and 2 - 21 °C during spring and summer (May-Aug, Fig. 3) at LM compared to -5 and 0.5 °C and 0 - 15 °C, respectively, at UM. During the spring, the soil was substantially warmer at LM than at UM, which led to earlier snowmelt. The average April-June soil temperature at the LM site reached 7.0 - 7.3 °C during the study period, compared to only 4.0 - 5.4 °C at UM. Notably in 2022, the soil temperature at LM reached 5 °C almost a month earlier than at UM, which would have allowed the trees to start transpiring earlier, although we do not have transpiration data prior to May which could confirm this. These results highlight an important indirect impact of the fire: the loss of the forest floor and understory vegetation can cause an earlier start of the growing season at the LM site, which increases water usage by the trees and evaporation of water from the soil surface and could make them more vulnerable to drought. On the other hand, reduced competition for water from the forest floor vegetation may improve water availability for the trees. At the LM site some trees maintained a high or even higher sap flux density than those at the unburnt site (Fig. 5), which could be related to this increased access to water.

The soil water content (VWC) at LM declined with each year since the fire relative to UM (Fig. 3). We measured VWC relatively close to the surface and it has been shown that 70 % of water uptake by pine trees originates from shallow soil layers (Song et al., 2016). However, since pine trees may also use water from deeper soil layers in periods of reduced water availability, we cannot deduce unequivocally whether the differences in sap flux density between the burnt and unburnt forest sites were due to fire-related changes in VWC and soil temperature or whether the fire-affected trees responded differently to soil moisture availability.

4.3. Differences in tree stem increment and tree ring width

The tree ring width (TRW) chronologies suggest that the two sites may have responded differently to variations in the climate in the decades before the fire. There are many possible underlying factors for these growth deviations. Firstly, the trees at UM are slightly younger than at LM, which can result in stronger influence of juvenile growth in the TRW. Additionally, as the tree replication in the two TRW chronologies is relatively low, growth deviations in individual trees could have a disproportionately large impact on the final TRW chronologies. The two sites may also have been managed differently; for example thinning at one of the sites may cause growth patterns of the trees to differ at the sites, even if the climatological factors are the same. However, apart from the 2018 fire, no such growth disturbances are known at our sites for the past decade, the growth variations in the TRW chronology and in the dendrometer data after 2018 are related to the forest fire.

Tree stem increment (measured by the dendrometers) differed between the sites, with lower total seasonal growth at LM compared to UM, especially in 2020 and 2022. An explanation for the difference in stem increment between the sites is that at LM, fine roots damaged by the fire needed to be rebuilt (Świątek and Pietrzykowski, 2021). Therefore, assimilated carbon may have been mostly invested in carbon belowground rather than stored in the stem, to compensate for the loss of roots during the fire. As a result, stem growth after the fire was lower at LM than at UM. This is also supported by a continuous decline in the tree ring width (growth) at LM since the fire. Similarly, a study of Scots Pine in Norway showed that forest fire led to a slight and temporary reduction in tree growth five years after the fire, followed by an increase in growth 11–20 years after the fire (Blanck et al., 2013). Further, WUE fluctuated significantly at LM between 2020–2022, whereas a gradual increase in WUE was observed for UM. Declines in WUE at LM indicate

that the trees were assimilating less carbon per unit of water transpired and are further evidence that the trees were allocating carbon to rebuilding lost root mass rather than to stem growth. These results highlight the need for long-term monitoring of stem increment of trees after fire as fire can cause changes in carbon allocation within the affected trees over several years.

In addition, at the LM site, there was a lower magnitude of reversible shrinkage and swelling of the stem at the daily scale than at UM, especially during the dry period in August 2020. These differences in stem reversible shrinkage and swelling might be related to different management of water stored in the stem. It has been shown that maximum daily stem shrinkage corresponds to the difference between water demand and water supply (Zweifel et al., 2000; Güney et al., 2020). Larger stem increment variations at daily to weekly time scales usually imply that trees are using stem water for transpiration whereas less variation may suggest less effective stem water storage. This may mean that after low-severity fire, trees are slower at replenishing stems with available water during alternating drier and wetter periods. Moreover, the lower magnitude of reversible shrinkage and swelling of the LM trees could have been caused by injury of the living cells within the sapwood and the phloem. Lintunen et al. (2017) found that damage to living cells impacts their water storage capacity which results in reduced diameter changes of branches. This confirms the vulnerability of forests affected by low-severity fires to changing environmental conditions, even if the fire has not resulted in immediate tree mortality.

Our measurements of tree stem increment, reversible stem shrinkage and swelling, and sap flow provide valuable information on stand conditions. The differences in stand conditions that we observed between unburnt and burnt sites for the same meteorological and soil properties suggest that fire-affected trees are functioning, but need several years to recover from the low-severity fire. A longer measurement series would help to quantify the longevity of these legacy impacts of fire on the trees at LM. Further work is needed to capture the effects of low-severity fire on sap flow and tree growth in other boreal forests to ascertain whether our results are applicable to the wider boreal forest region.

5. Conclusions

In this study, we investigated the recovery dynamics of a boreal *Pinus sylvestris* forest stand after a low-severity fire in 2018 and compared it with an adjacent unburnt stand. We analysed transpiration (sap flux density) and stem increment fluctuations over a three-year period (2020–2022), two to four years after the fire. Although the fire did not kill the trees nor affect the tree canopy, sap flux density was more variable, and in some cases lower in the fire-affected trees than in the unburnt trees. Differences between measured sap flux density at both stands decreased in the third post-fire growing season, but larger differences emerged in the fourth growing season after the fire, indicating a substantial inter-annual variability in recovery dynamics. The fire-affected trees had consistently lower cambial growth rates than those at the unburnt stand, demonstrating that this low-severity fire had significantly affected tree growth dynamics and tree carbon allocation. Our results suggest that trees impacted by low-severity fire are less resistant to disturbances such as water shortages and prioritize allocation of carbon to roots to repair fire-related damage over stem growth.

Studies of sap flow after fire are still rare. Our results indicate that sap flow and stem increment measurements provide valuable information on the forest health status. The differences we observed between the burnt and unburnt sites with the same meteorological and soil properties highlight that the consequences of fire on tree growth are visible for multiple years after a fire. Continuous and long-term observation of changes in tree water and carbon management will reveal the time needed for complete recovery.

CRediT authorship contribution statement

Paulina Dukat: Formal analysis, Investigation, Visualization, Writing – original draft, Writing – review & editing. **Julia Kelly:** Investigation, Writing – review & editing. **Stefan H. Doerr:** Writing – review & editing, Funding acquisition. **Johannes Edvardsson:** Investigation, Writing – review & editing. **Teemu S. Hölttä:** Writing – review & editing, Funding acquisition. **Irene Lehner:** Investigation. **Anders Lindroth:** Conceptualization, Methodology, Writing – review & editing, Funding acquisition. **Cristina Santín:** Writing – review & editing, Funding acquisition. **Natascha Kljun:** Conceptualization, Methodology, Investigation, Resources, Writing – review & editing, Supervision, Project administration, Funding acquisition.

Declaration of competing interest

The authors declare that they have no known competing financial interests or personal relationships that could have appeared to influence the work reported in this paper.

Data availability

Data will be made available on request.

Acknowledgements

This research was funded by FORMAS grants #2018-02700 and 2019-00836, and the Crafoord foundation grant 20190763. We thank Jukka Kuivaniemi for his support in accessing and establishing the sites. We are also grateful to Ellinor Delin, Margarida Soares, and Jonas Nilsson for their help conducting the vegetation surveys. The work was done in collaboration with the University of Helsinki in the framework of the project 342930 of the Academy of Finland and with Poznan university of Life Sciences in the framework of the project by General Directorate of the State Forests, Warsaw, Poland (project name: LAS IV 31/2021/B; contract no. EZ.271.3.3.2021).

Supplementary materials

Supplementary material associated with this article can be found, in the online version, at doi:10.1016/j.agrformet.2024.109899.

References

Amiro, BD, Ian MacPherson, J, Desjardins, RL, Chen, JM, Liu, J, 2003. Post-fire carbon dioxide fluxes in the western Canadian boreal forest: evidence from towers, aircraft and remote sensing. Agric. For. Meteorol. 115, 91–107.

Bär, A, Nardini, A, Mayr, S., 2018. Post-fire effects in xylem hydraulics of Picea abies, Pinus sylvestris and Fagus sylvatica. New Phytol. 217, 1484–1493.

Bär, A, Michaletz, ST, Mayr, S., 2019. Fire effects on tree physiology. New Phytol. 223, 1728–1741.

Balfour, DA, Midgley, JJ, 2006. Fire induced stem death in an African acacia is not caused by canopy scorching. Austral Ecol. 31, 892–896.

Blanck, YL, Rolstad, J, Storaunet, KO., 2013. Low- to moderate-severity historical fires promoted high tree growth in a boreal Scots pine forest of Norway. Scand. J. Forest Res. 28, 126–135.

Bova, AS, Dickinson, MB., 2005. Linking surface-fire behavior, stem heating, and tissue necrosis. Canad. J. Forest Res. 35, 814–822.

Bräker, OU., 2002. Measuring and data processing in tree-ring research—a methodological introduction. Dendrochronologia 20, 203–216.

Bremond, L, Carcaillet, C, Favier, C, Ali, AA, Paitre, Ć, Bgin, Y, Bergeron, Y, Richard, PJH., 2010. Effects of vegetation zones and climatic changes on fire-induced atmospheric carbon emissions: a model based on paleodata. Int. J. Wildland. Fire 19, 1015–1025.

Bryant, KN, Stenzel, J, Mathias, J, Kwon, H, Kolden, CA, Lynch, L, Hudiburg, T., 2022. Boosts in leaf-level photosynthetic capacity aid Pinus ponderosa recovery from wildfire. Environ. Res. Lett. 17, 114034.

Butler, BW, Webb, BW, Jimenez, D, Reardon, JA, Jones, JL., 2005. Thermally induced bark swelling in four North American tree species. Canad. J. Forest Res. 35, 452–460.

Čermák, J, Deml, M., 1974. Method of Water Transport Measurements in Woody Species, Especially in Adult Trees (in Czech). Patent (Certification of authorship).
Čermak, J, Deml, M, Penka, M., 1973. A new method of sap flow rate determination in trees. Biol. Plant 15, 171–178.
Čermák, J, Kučera, J, Nadezhdina, N., 2004. Sap flow measurements with some thermodynamic methods, flow integration within trees and scaling up from sample trees to entire forest stands. Trees 18, 529–546.
Christensen-Dalsgaard, KK, Tyree, MT, 2014. Frost fatigue and spring recovery of xylem vessels in three diffuse-porous trees in situ. Plant Cell Environ. 37, 1074–1085.
Cook, ER, Holmes, RL., 1984. Program ARSTAN User Manual: Laboratory of Tree Ring Research. University of Arizona, Tucson.
Cook, ER, Kairiukstis, LA., 1990. Methods of Dendrochronology, Applications in the Environmental Sciences. Kluwer Academic Publishers, International Institute for Applied Systems Analysis, London.
Cook, ER, Krusic, PJ., 2006. ARSTAN_41: a Tree-Ring Standardization Program Based On Detrending and Autoregressive Time Series Modeling, with Interactive Graphics. Lamont Doherty Earth Observatory of Columbia University. In Press.
de Groot, WJ, Cantin, AS, Flannigan, MD, Soja, AJ, Gowman, LM, Newbery, A., 2013. A comparison of Canadian and Russian boreal forest fire regimes. For. Ecol. Manage 294, 23–34.
Delin, E., 2021. MSc Thesis. University of Gothenburg.
Deslauriers, A, Rossi, S, Anfodillo, T., 2007. Dendrometer and intra-annual tree growth: what kind of information can be inferred? Dendrochronologia 25, 113–124.
Dickinson, MB, Johnson, EA., 2001. Fire effects on trees. Forest Fires 477–525.
Ducrey, M, Duhoux, F, Huc, R, Rigolot, E., 1996. The ecophysiological and growth responses of Aleppo pine (Pinus halepensis) to controlled heating applied to the base of the trunk. Canad. J. Forest Res. 26, 1366–1374.
Dukat, P, Ziemblińska, K, Olejnik, J, Małek, S, Vesala, T, Urbaniak, M., 2021. Estimation of biomass increase and cue at a young temperate scots pine stand concerning drought occurrence by combining eddy covariance and biometric methods. Forests. 12, 1–20.
Faber-Langendoen, D, Davis, MA., 1995. Effects of fire frequency on tree canopy cover at Allison Savanna, eastcentral Minnesota, USA. Natur. Areas J. 15, 319–328.
Ferrat, L, Morandini, F, Lapa, G., 2021. Influence of prescribed burning on a pinus nigra subsp. Laricio forest: Heat transfer and tree vitality. Forests 12.
Flanagan, NE, Wang, H, Winton, S, Richardson, CJ., 2020. Low-severity fire as a mechanism of organic matter protection in global peatlands: thermal alteration slows decomposition. Glob. Change Biol. 26, 3930–3946.
Friedman, JH., 1984. A Variable Span Smoother. Department of Statistics Technical Report LCS 5, Stanford.
Fritts, HC., 1976. Tree Rings and Climate. Academic, London.
Güney, A, Zweifel, R, Türkan, S, Zimmermann, R, Wachendorf, M, Güney, CO., 2020. Drought responses and their effects on radial stem growth of two co-occurring conifer species in the Mediterranean mountain range. Ann. For. Sci. 77.
Gielen, B, Acosta, M, Altimir, N, et al., 2018. Ancillary vegetation measurements at ICOS ecosystem stations. Int. Agrophys. 32, 645–664.
Girardin, MP, Bergeron, Y, Tardif, JC, Gauthier, S, Flannigan, MD, Mudelsee, M., 2006. A 229-year dendroclimatic-inferred record of forest fire activity for the Boreal Shield of Canada. Int. J. Wildland. Fire 15, 375–388.
Kelly, J, Ibáñez, TS, Santín, C, Doerr, SH, Nilsson, MC, Holst, T, Lindroth, A, Kljun, N., 2021. Boreal forest soil carbon fluxes one year after a wildfire: effects of burn severity and management. Glob. Chang. Biol. 27, 4181–4195.
Kolari, P, Chan, T, Porcar-Castell, A, Bäck, J, Nikinmaa, E, Juurola, E, 2014. Field and controlled environment measurements show strong seasonal acclimation in photosynthesis and respiration potential in boreal Scots pine. Front. Plant Sci. 5.
Kučera, J, Vaníčček, R, Urban, J., 2020. Automated exponential feedback weighting method for subtraction of heat losses from sap flow measured by the trunk heat balance method. Acta Hortic., pp. 81–88.
Kučera, J– EMS, 2018. Sap flow system EMS 81 User Manual. *in press*.
Kucera, J, Cermák, J, Penka, M., 1977. Improved thermal method of continual recording the transpiration flow rate dynamics. Biol. Plant 19, 413–420.
Le Goff, H, Flannigan, MD, Bergeron, Y, Girardin, MP, 2007. Historical fire regime shifts related to climate teleconnections in the Waswanipi area, central Quebec, Canada. Int. J. Wildland Fire 16, 607–618.
Lintunen, A, Lindfors, L, Nikinmaa, E, Hölttä, T., 2017. Xylem diameter changes during osmotic stress, desiccation and freezing in Pinus sylvestris and Populus tremula. Tree Physiol. 37, 491–500.
Marklund, LG., 1988. *Biomass Functions for Pine, Spruce and Birch in Sweden*. Report 45, Dept. Forest Survey., Umea.
Mayr, S, Cochard, H, Améglio, T, Kikuta, SB., 2007. Embolism formation during freezing in the wood of Picea abies. Plant Physiol. 143, 60–67.
Michaletz, ST, Johnson, EA., 2007. How forest fires kill trees: a review of the fundamental biophysical processes. Scand. J. Forest Res. 22, 500–515.
Michaletz, ST, Johnson, EA, Tyree, MT, 2012. Moving beyond the cambium necrosis hypothesis of post-fire tree mortality: cavitation and deformation of xylem in forest fires. New Phytol. 194, 254–263.
Niu, CY, Meinzer, FC, Hao, GY., 2017. Divergence in strategies for coping with winter embolism among co-occurring temperate tree species: the role of positive xylem pressure, wood type and tree stature. Funct. Ecol. 31, 1550–1560.
Nolan, RH, Lane, PNJ, Benyon, RG, Bradstock, RA, Mitchell, PJ., 2014. Changes in evapotranspiration following wildfire in resprouting eucalypt forests. Ecohydrology 7, 1363–1377.
Obojes, N, Meurer, A, Newesely, C, Tasser, E, Oberhuber, W, Mayr, S, Tappeiner, U., 2018. Water stress limits transpiration and growth of European larch up to the lower subalpine belt in an inner-alpine dry valley. New Phytol. 220, 460–475.
Partelli-Feltrin, R, Smith, AMS, Adams, HD, Thompson, RA, Kolden, CA, Yedinak, KM, Johnson, DM., 2022. Death from Hunger or Thirst? Phloem Death, Rather Than Xylem Hydraulic Failure, as a Driver of Fire-Induced Conifer Mortality.
Persson, H., 1980. Death and replacement of fine roots in a mature scots pine stand. Ecological Bulletins - Structure and Function of Northern Coniferous Forests: An Ecosystem Study, pp. 251–260.
Peterken, GF., 2001. Natural Woodland: Ecology and Conservation in Northern Temperate Regions. Cambridge University Press.
Peterson, DL, Ryan, KC., 1986. Modeling postfire conifer mortality for long-range planning. Environ. Manage 10, 797–808.
Petersson, H, Ståhl, G., 2006. Functions for below-ground biomass of Pinus sylvestris, Picea abies, Betula pendula and Betula pubescens in Sweden. Scand. J. Forest Res. 21, 84–93.
Ponomarev, EI, Kharuk, VI, Ranson, KJ., 2016. Wildfires dynamics in Siberian larch forests. Forests. 7.
Renninger, HJ, Clark, KL, Skowronski, N, Schäfer, KVR., 2013. Effects of a prescribed fire on water use and photosynthetic capacity of pitch pines. Trees 27, 1115–1127.
Rinn, F., 2003. TSAP-Win User Reference Manual. Rinntech, Heidelberg.
Santín, C, Doerr, SH., 2016. Fire effects on soils: the human dimension. Philos. Trans. R. Soc. B 371, 28–34.
SMHI, 2022. SMHI. https://www.smhi.se/data/meteorologi/ladda-ner-meteorologiska-observationer#param=airtemperatureInstant,stations=core.
Smith, HG, Sheridan, GJ, Lane, PNJ, Nyman, P, Haydon, S, 2011. Wildfire effects on water quality in forest catchments: a review with implications for water supply. J. Hydrol. 396, 170–192.
Song, L, Zhu, J, Li, M, Zhang, J, Lv, L., 2016. Sources of water used by Pinus sylvestris var. mongolica trees based on stable isotope measurements in a semiarid sandy region of Northeast China. Agric. Water. Manage 164, 281–290.
Swezy, DM, Agee, JK., 1991. Prescribed-fire effects on fine-root and tree mortality in old-growth ponderosa pine. Can. J. For. Res 626–634.
Świątek, B, Pietrzykowski, M., 2021. Soil factors determining the fine-root biomass in soil regeneration after a post-fire and soil reconstruction in reclaimed post-mining sites under different tree species. Catena 204.
Szatniewska J, Zavadilova I, Krejza J, Petrik P, Stojanovi M. 2022a. Forest Ecology and Management Species-specific growth and transpiration response to changing environmental conditions in floodplain forest. 516.
Szatniewska, J, Zavadilova, I, Nezval, O, Krejza, J, Petrik, P, Čater, M, Stojanović, M., 2022b. Species-specific growth and transpiration response to changing environmental conditions in floodplain forest. For. Ecol. Manage 516.
Tecle, A, Neary, D., 2015. Water quality impacts of forest fires. J. Pollut. Effects Control 03.
Uhl, C, Kauffman, JB., 1990. Deforestation, fire susceptibility, and potential tree responses to fire in the eastern Amazon. Ecology. 71, 437–449.
Valverde-Barrantes, OJ., 2022. Dissecting how fine roots function. New Phytol. 233, 1539–1541.
Vanguelova, EI, Nortcliff, S, Moffat, AJ, Kennedy, F., 2005. Morphology, biomass and nutrient status of fine roots of Scots pine (Pinus sylvestris) as influenced by seasonal fluctuations in soil moisture and soil solution chemistry. Plant Soil. 270, 233–247.
Varner, JM, Hood, SM, Aubrey, DP, Yedinak, K, Hiers, JK, Jolly, WM, Shearman, TM, McDaniel, JK, O'Brien, JJ, Rowell, EM, 2021. Tree crown injury from wildland fires: causes, measurement and ecological and physiological consequences. New Phytol. 231, 1676–1685.
Vertessy, RA, Watson, FGR, O'Sullivan, SK., 2001. Factors determining relations between stand age and catchment water balance in mountain ash forests. For. Ecol. Manage 143, 13–26.
Walker, XJ, Baltzer, JL, Cumming, SG, et al., 2019. Increasing wildfires threaten historic carbon sink of boreal forest soils. Nature 572, 520–523.
West, AG, Nel, JA, Bond, WJ, Midgley, JJ., 2016. Experimental evidence for heat plume-induced cavitation and xylem deformation as a mechanism of rapid post-fire tree mortality. New Phytol. 211, 828–838.
Zeppel, MJB, Anderegg, WRL, Adams, HD, Hudson, P, Cook, A, Rumman, R, Eamus, D, Tissue, DT, Pacala, SW., 2019. Embolism recovery strategies and nocturnal water loss across species influenced by biogeographic origin. Ecol. Evol. 9, 5348–5361.
Zheng, B, Ciais, P, Chevallier, F, et al., 2023. Record-high CO2 emissions from boreal fires in 2021. Science 379, 912–917.
Zweifel, R, Item, H, Häsler, R., 2000. Stem radius changes and their relation to stored water in stems of young Norway spruce trees. Trees 15, 50–57.
Zweifel, R, Eugster, W, Etzold, S, Dobbertin, M, Buchmann, N, Häsler, R., 2010. Link between continuous stem radius changes and net ecosystem productivity of a subalpine Norway spruce forest in the Swiss Alps. New Phytol. 187, 819–830.